Applied Energy 99 (2012) 344–354

Contents lists available at SciVerse ScienceDirect

Applied Energy

journal homepage: www.elsevier.com/locate/apenergy

Co-firing based on biomass torrefaction in a pulverized coal boiler with aim of 100% fuel switching

Jun Li [a,*], Artur Brzdekiewicz [b], Weihong Yang [a], Wlodzimierz Blasiak [a]

[a] Division of Energy and Furnace Technology, Royal Institute of Technology (KTH), Brinellvägen 23, 10044 Stockholm, Sweden
[b] Remak-Rozruch SA, Opole, Poland

HIGHLIGHTS

- ▶ Torrefaction based co-firing system was proposed.
- ▶ The kinetics of torrefied biomass has been investigated experimentally.
- ▶ The performances of co-firing with varying biomass substitutions have been studied.
- ▶ No obvious reduction of boiler load was found when 100% coal switched to biomass.
- ▶ Net CO_2 and NO_x emissions reduced with increasing of biomass substitutions.

ARTICLE INFO

Article history:
Received 31 March 2012
Received in revised form 10 May 2012
Accepted 20 May 2012
Available online 26 June 2012

Keywords:
Co-firing
Torrefaction
Biomass
CFD
Pulverized coal boiler

ABSTRACT

Torrefied biomass has several benefits, such as higher energy density, good grindability, higher flowability and uniformity. The process of torrefaction moves the chemical and physical properties of raw biomass close to that of bituminous coal, which allows co-utilization with high substitution ratios of biomass in the existing coal-fired boilers without major modifications. In this study, a torrefaction based co-firing system was proposed and studied. Devolatilization and char oxidize kinetics of the torrefied biomass have been investigated experimentally. CFD modeling of co-firing with varying substitutions of torrefied biomass in a pulverized coal boiler have been carried out. To figure out the boiler performance when co-firing torrefied biomass, five different cases were involved and simulated, coal only, 25% biomass, 50% biomass, 75% biomass, and 100% biomass on thermal basis, respectively. The results showed torrefaction is able to provide a technical option for high substitution ratios of biomass in the co-firing system. The case-study pulverized coal boiler could be fired 100% torrefied biomass without obvious decreasing of the boiler efficiency and fluctuation of boiler load. More positively, the net CO_2 and the NO_x emissions significantly reduced with increasing of biomass substitutions in the co-firing system.

© 2012 Elsevier Ltd. All rights reserved.

1. Introduction

Co-firing biomass with coal in traditional coal-fired boilers for electricity production represents a cost effective and efficient renewable option that promises reduction in effective CO_2 emissions, reduction in NO_x emissions, and several societal benefits [1,2]. Many different types of biomass can be co-fired with coal, such as wood, residues from forestry and related industries, agricultural residues, and various biomasses in refined form such as pellets. Biomass is able to penetrate all energy sector markets, but technical and economic constraints still limit its general deployment. Currently, technical challenges associated with co-firing are: (1) cost-effective methods for getting more and wider varieties of fuels into the boiler, (2) occurrence of insufficient gas mixing or stratified flows in the boiler, (3) fouling and corrosion of the boiler, (4) continuation of fly ash utilization, and (5) impacts on performance of the flue gas cleaning. The economics of biomass co-firing are significantly impacted by the twin factors of deregulation and environmental requirement. Those non-technical barriers are as follows: (1) lacking of financial incentives, and uncertain fuel price/availability, (2) legislative aspects (utilization of fly ash in cement, determining green share of electricity produced, and unclean emission legislation), (3) public perception of co-firing of biomass/waste, and (4) getting the permits through. Uncertainties in both arenas make investment in most, or all, biomass co-firing technologies difficult to justify. Therefore, it is expected an efficient but sustainable biomass thermal conversion schemes. Further on, new EU regulations force power sectors to use more biomass, such as Large Combustion Plant Directive (LCPD), National Emission

---

* Corresponding author. Tel.: +46 8 7908402; fax: +46 8 20 76 81.
E-mail address: jun2@kth.se (J. Li).

0306-2619/$ - see front matter © 2012 Elsevier Ltd. All rights reserved.
http://dx.doi.org/10.1016/j.apenergy.2012.05.046

Nomenclature

A	pre-exponential factor for char oxidation (s^{-1})
A_i	pre-exponential factor for devolatilization (s^{-1})
C	carbon content in solid fuel (wt.%, daf)
C_D	drag force coefficient
C_{SW}	swelling factor
d_p	current particle diameter (m)
$d_{p,0}$	initial particle diameter (m)
D_0	diffusion rate coefficient (m^2/s)
E_c	the activation energy of char oxidation (kJ/mol)
E_i	activation energy of devolatilization(kJ/mol)
$f_{v,0}$	the fraction of volatiles in the particle
$f_{w,0}$	the fraction of moisture in the particle
g	gravity acceleration constant, 9.8 m/s^2
H	hydrogen content in solid fuel (wt.%, daf)
m_p	particle mass (kg)
$m_{p,0}$	initial particle mass (kg)
O	oxygen content in solid fuel (wt.%, daf)
Re	Reynolds number
T_m	mean particle and gas temperature (K)
V_i	volatile yield factor

Greek symbols

ρ_p	particle density (kg/m^3)
ρ	fluid phase density (kg/m^3)
μ_p	particle velocity (m/s)
μ	fluid phase velocity (m/s)

Ceilings Directive (NECD), and Integrated Pollution Prevention and Control Directive (IPPCD) [3]. Those regulations further promote large percentage biomass will be used by power sectors.

The co-firing technologies employed in power sector are broadly classified into three types: direct co-firing, indirect co-firing, and gasification based co-firing [4,5]. In direct co-firing system, the biomass is feed into the mills to be firstly pulverized as biomass powder in the mill system, and then introduced into boiler either separately or blend with coal [6–8]. Indirect co-firing involves the installation of a completely separate biomass boiler to produce low-grade steam for utilization in the coal-fired power plant prior to being upgraded, resulting in higher conversion efficiencies [4]. Gasification based co-firing system involves the gasification of solid biomass and combustion of the product fuel gas in the furnace of the coal-fired boiler, and offers a high degree of fuel flexibility [9–11]. Currently, direct co-firing is the most popular option for biomass applications in industry, due to the relatively low investment cost of turning an existing coal power plant to a co-firing plant [4,12]. However, the majority of direct co-firing installations were operated with less than 10% (thermal basis) of biomass co-firing ratios, since the technical and economic constraints [4,5].

2. Torrefaction based co-firing system

2.1. Concept of torrefaction based co-firing system

In order to increase the possibility of co-firing application of biomass, the torrefaction as a pre-treatment technology for co-firing was reported by the Energy Research Centre of the Netherlands (ECN) in 2005, which makes biomass is able to compete with fossil fuels, and thus provides an option for the direct co-firing with a large percentage of biomass without major threats [13].

Torrefaction is a thermo-chemical process conducted at 200–300 °C, typically, 1-h residence time, during which biomass partially decomposes giving off volatiles and producing the remaining solid as a final product [12,14]. Loss of the tenacious nature of raw biomass is mainly coupled to the breakdown of hemicellulose matrix, which bonds the cellulose fibers in the raw biomass, and decrease the length of these fibers during the depolymerization process [15]. Generally, torrefied biomass has several benefits [13–18]. First, torrefied biomass contains, typically, 70% of its initial weight and 90% of the original energy content [19]. As the result, the energy density of biomass increases about 1.3 times after torrefaction process, so that the stability of the boiler loads can be achieved, and the transportation cost of torrefied biomass will be also reduced about 1.3 times. Moreover, the higher fibrous in raw biomass makes the grinding of the raw sample difficult and energy consuming [14]. Compared with the raw biomass, torrefied biomass can be characterized by the anhydrous weight loss, and the grinding energy greatly decreases with weight losing [20]. For example, a reduction of 85% of power consumption was maximally observed for torrefied willow [21]. Thirdly, in contrast to the raw biomass, torrefied wood particles have higher flowability and good fluidization behavior, which is an important performance for an easy injection of biomass powder into boiler, because the torrefied biomass has a brittle behavior with decreased strength, smaller particles sizes, and lower moisture content. Finally, torrefied biomass has an increased uniformity in product quality. For instance, it has been found that woodcuttings, demolition wood, waste wood have quite similar physical and chemical properties after torrefaction, so that it is possible to use a wide range of fuels and reduces season influences [13]. Accordingly, the promising chemical and physical properties of torrefied biomass provide a co-utilization option with high ratios of biomass in existing coal-fired boilers without major modifications. However, the combustion behavior, operation performance and emissions of co-firing system based on biomass torrefaction are not clear.

In this study, the torrefaction based co-firing system in pulverized coal boilers has been proposed with the aim of 100% fuel switching, as schemed in Fig. 1. Raw biomass was pretreated by torrefaction process previously and the torrefied biomass was grinded in the existing but separate coal-mills to produce the biomass powders, which were finally introduced into combustion chamber by primary air. Torrefied biomass powders were then combusted separately in the upper burners when in co-firing cases. The bottom burners are designed either for coal particles or biomass particles, which can be switched to use biomass only in the pure biomass combustion cases, as shown in Fig. 1. To figure out the performance of co-firing torrefied biomass in a front-wall pulverized coal boiler, five different cases were involved and simulated, coal only, 25% biomass, 50% biomass, 75% biomass and 100% biomass cases respectively. In which, the substitution ratios of biomass are on thermal basis, and the 100% coal case has been selected as the base case for validation. More detailed investigations covering the profiles of temperature, major gas components, pollutants and unburned carbons have been done. The results of numerical analysis with aim of 100% fuel switching were discussed in this paper.

2.2. Fuel properties of torrefied biomass

In this work, torrefaction process has been done previously to get torrefied biomass, which derived from its raw biomass with 20% of volatile content releases on dry basis. Proximate and ultimate analysis data of raw biomass, torrefied biomass and coal

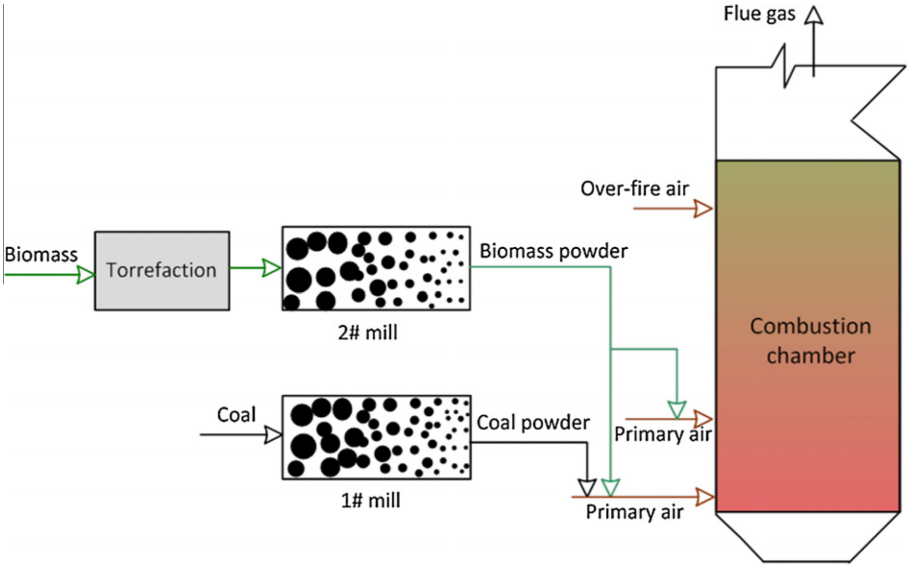

Fig. 1. Scheme of torrefaction based co-firing system.

Table 1
Analysis data of raw biomass, torrefied biomass and coal particles.

	Units	Raw biomass	Torrefied biomass	Coal
Moisture	4.2	4.2	5.6	1.43
Proximate analysis (dry basis)				
Ash	1.95 wt.%	1.95	7.31	25.06
Volatile	79.72 wt.%	79.72	61.87	27.85
Char	18.33 wt.%	18.33	30.82	47.09
LHV	18.0 MJ/kg	18.0	20.5	24.0
Ultimate analysis (dry basis)				
C	50.32 wt.%	50.32	55.43	60.26
H	6.02 wt.%	6.02	4.90	3.97
O	41.42 wt.%	41.42	31.83	8.33
N	0.26 wt.%	0.26	0.50	1.27
S	0.03 wt.%	0.03	0.04	1.11

particles are listed in Table 1. The proximate analysis confirms that the torrefaction dramatically reduced the volatile to fixed carbon ratio and improves the energy density. Moisture content of the raw material is lower than the torrefied material, which could be caused by the different origin of the material.

The Van Krevelen diagram gives the relation between O/C and H/C for different solid fuels, as shown in Fig. 2. In which, the torrefied biomass and coal were studied in this work; the bituminous, sub-bituminous and raw biomasses are used for reference. From Fig. 2, obviously, the raw biomass has lower energy density than coal. However, promisingly, it shows that torrefaction changes the elementary composition of biomass and moves it towards coal. Besides, breakdown of hemicellulose matrix with weakening of the tenacious nature of the biomass, which bonds the cellulose fibers in biomass, and decrease the length of these fibers during depolymerization process. Therefore, torrefied biomass is able to be grinded by the existing coal milling systems without modifications.

Co-firing a biofuel in existing pulverized-coal fired boilers sets high demands for grinding of biomass [6]. The critical factor is the particle size of the biomass, which is necessary to ensure proper combustion efficiency and a stable flame. In this work, after torrefaction, it is assumed that biomass was grinded separately by an existing coal-mill. Then the biomass particles and coal particles sieved and selected were in same range of 62–150 μm.

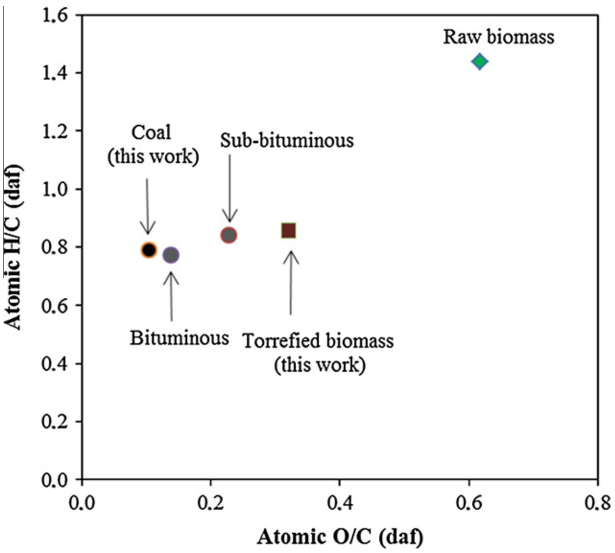

Fig. 2. Van Krevelen diagram for different solid fuel (*Note*: (1) Raw biomass is the parent species of torrefied biomass; (2) The reference data of bituminous and sub-bituminous are from IFRF data bank).

2.3. Experimental studies of torrefied biomass

2.3.1. TG and DTG tests

To further identify the advances of chemical properties of torrefied biomass, thermogravimetric tests were performed under inert or atmosphere conditions. In this work, the operating procedure includes, dry process, which is a heating process with constant heating rate (20 °C/min) from room temperature to 105 °C under nitrogen, and then maintains the isothermal period at 105 °C about 10 min; pyrolysis process, which is also a heating process with constant heating rate (20 °C/min) from 105 to 900 °C under nitrogen, and then maintains the isothermal period at 900 °C about 10 min; char oxidized process, which starts nitrogen cooling period from 900 to 800 °C under nitrogen gas, and then switches from nitrogen to air, and maintains the isothermal period for 10 min under air.

2.3.2. Kinetics tests

To obtain more realistic kinetics data, devolatilization tests at higher heating rate were carried out in an isothermal plug flow reactor (IPFR) [22]. The test conditions were set similar to industrial pulverized fuel applications, such as high temperature and high heating rate. The reactor is possible used to represent conditions found in full-scale combustion processes with heating rates on the order of 10^4–10^5 °C/s, maximum temperature of 1400 °C, and particle residence time between 5 and 1500 ms. A flow of 100 g/h of biomass powder was guaranteed to maintain stationary conditions for a time test of at least 30 min. The fuel conversion was evaluated by comparing the composition of the collected solid residue with that of the parent fuel by means of the ash tracer method.

After devolatilization under the nominal temperature of 900 °C and residence time of 300 ms conditions that assure the complete devolatilization but prevent the graphitization of the carbonaceous matrix, the char of torrefied biomass obtained have been tested in the ThermoGravimetric Balance to evaluate the char oxidation kinetics. Small char samples (3 mg) have been tested in order to limit material and thermal resistances during the tests. Three-time tests with a constant heating rate (20 °C/min) were carried out [22].

3. Description of boiler and operating conditions, and modeling

3.1. Boiler introduction

The case-study boiler, OP-650, is a front-wall pulverized coal boiler with maximum electricity production capacity of 220 MWe. In this work, the full boiler geometry was modeled, and the cross sectional area of domain was $15.598 \times 8.958\ \mathrm{m}^2$ and the height of the domain was 39.453 m, as shown in Fig. 3. The mesh system consisted of 796,372 structured hexahedral cells. The mesh was refined at the location of the burners, where the ignition and most of the combustion reactions occurred. The super-heaters on the top of boiler were also considered. There are 24 burners were arranged on front wall, all the burners as 4 rows and 6 burners equally spaced in each row. The amount of primary air controlled the rate of combustion in the chamber. The amount of secondary air controlled combustion efficiency. Sufficient OFA was added for the complete oxidation of any unburned combustibles and OFA ports were located on the rear wall, there were 10 injection nozzles. In addition, 8 vertical slots-air (front wall) and 2 rows protection-air (rear wall) were used for protecting the membrane walls against over temperature operation and influence of combustion products.

3.2. Operating conditions

In this work, five different cases were simulated and studied. One case of pure coal, three cases of co-firing with different substitution portions of biomass (25%, 50%, and 75% on thermal basis), and one case of pure biomass were modeled and studied. The operation data of 200 MWe pure coal case was collected in the power plant, as shown in Table 2. To obtain the operating parameters of three co-firing cases and the pure biomass case, several assumptions have been made based on the pure coal case: (1) total energy capacities are kept as 200 MWe, (2) total energy inputs of fuel are 513 MW/h, (3) the boiler operated with excess air ratios of 1.15, (4) all 24 burners are operated with average energy capacity and same conditions in all co-firing cases and the pure biomass case, (5) the portions of PA, SA, OFA, and protection air are kept same as the pure coal case. The operating parameters of all five cases are listed in Table 3.

Table 2
The operation parameters of boiler at 200 MWe.

Electrical power of block (MWe)	200
Boiler efficiency (%)	92.69
Pressure in the boiler drum (MPa)	14.15
Temperature in the boiler drum (°C)	336.5
Temperature of the feed water (°C)	240.9
Pressure of the feed water (MPa)	14.8
Capacity of the feed water (t/h)	569.6

3.3. Basic mathematical models

To obtain as precise as possible numerical analysis results, Solidworks software was used for the air supply system simulation to predict the velocity vectors and the temperature of combustion air. The details of air supply system simulations have been reported by Li et al. [23]. All the velocity vectors of combustion air obtained from the air system simulation were inputted as boundary conditions in Fluent by user-defined methods.

After the air supply system simulations, Ansys Fluent 13.0, was used to simulate combustion, fluid and particle flow, as well as heat and mass transfer inside the furnace [24]. The standard k-ε model with standard wall function was used for calculating the effect of turbulent flow inside furnace [25]. Lagrangian particle trajectories of the pulverized coal particles were calculated throughout the computational domain. The discrete ordinates (DOs) radiation model was used to simulate radiation heat transfer. Simulating coal combustion mainly involved the modeling of devolatilization, the homogeneous combustion of gaseous volatiles, and the heterogeneous oxidation of solid char particles [26]. The dry process, which is also important, starts with a progressive heating of the coal particle by convection and radiation. Wet combustion model was used for modeling the moisture release process during the heating stage [24].

Devolatilization is modeled to predict the volatile matter yield by the two-competing-rates model proposed by Kobayashi et al. [27] and the gas released during this process contributes to the gaseous reaction. The char combustion is computed according to the kinetics/diffusion-limited model [28,29], where the surface reaction rate is determined either by kinetics or by a diffusion rate. In practice, the operating temperature of furnace is high (above 1000 °C), so that volatile combustion happens at high Damköhler numbers ($\mathrm{Da} \gg 1$). Accordingly, the global reaction limited by diffusion was used for combustion of gaseous volatiles, and calculated by Eddy-Dissipation model [24]. For the torrefied biomass particles, the data for the kinetic rate of devolatilization and char oxidation were measured and presented in Table 4. For the coal particles, the kinetic parameters of devolatilization were obtained from Li et al. [30]; the kinetics of coal char oxidation were calculated based on Hurt and Mitchell's correlations [31]. Besides, diffusion coefficients for all cases were calculated based on $D_o = 2.53 \times 10^{-7} T_m^{0.75} / d_p$ [32].

3.4. NO_x formation modeling

Thermal NO_x is formed from oxidation of atmospheric nitrogen at relatively high temperatures in fuel-lean environments and has strong temperature dependence. The formation of thermal NO is determined by extended Zeldovich mechanism [33]. Fuel NO_x is formed from nitrogen bound in solid fuel, and the part of fuel-nitrogen is usually released as HCN and NH_3 accompanying with volatile releasing, which finally will be either oxidized into NO or reduced into N_2 [34]. For the coal, it is assumed that 90% of the nitrogen from the volatile will be converted to HCN, and the rest will form NH_3 [35]. While for biomass, oppositely, 90% of HCN and 10% of NH_3 were derived from the volatile [36]. Besides, in this

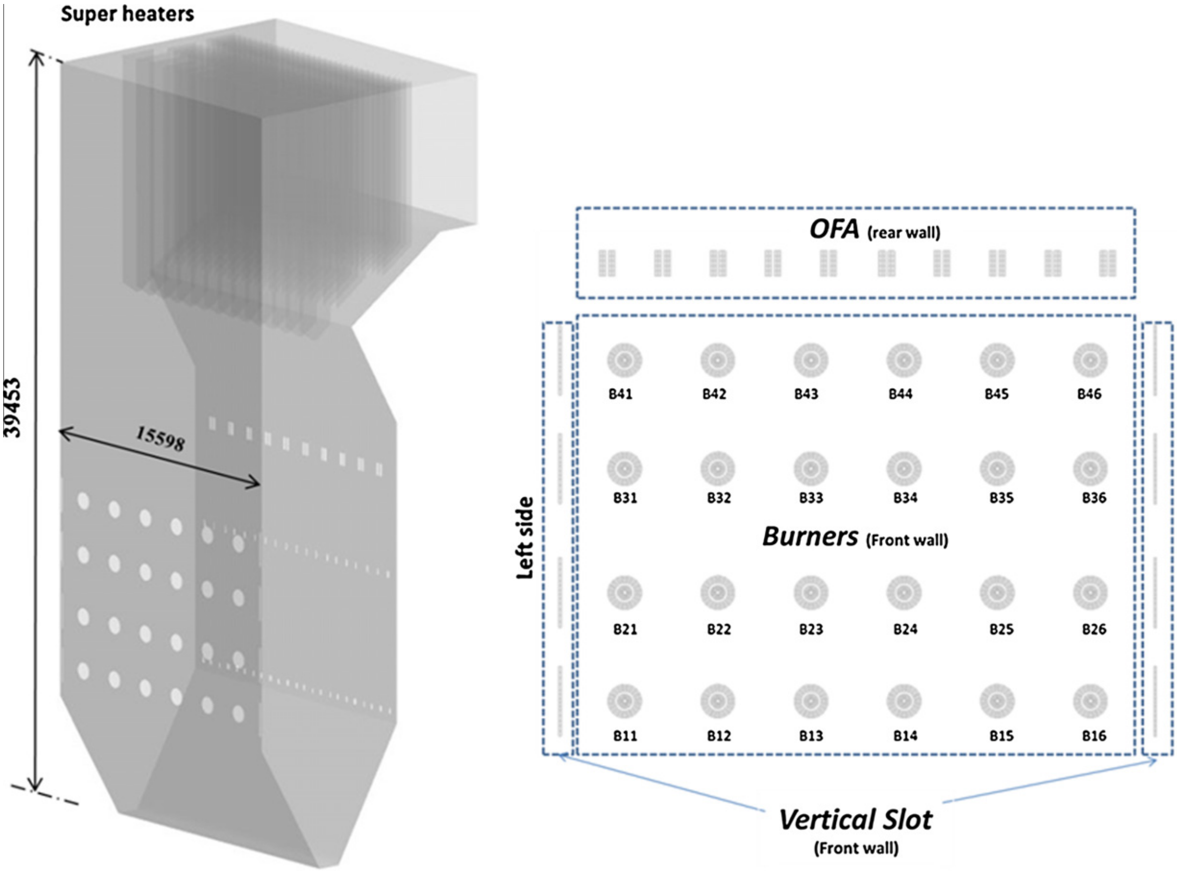

Fig. 3. Global geometry and grid structure of burners, OFA ports and vertical slots (dimensions in mm).

Table 3
The operating parameters of all five cases.

	Case 1	Case 2	Case 3	Case 4	Case 5
Combustion type	Pure coal	Co-firing	Co-firing	Co-firing	Pure biomass
Biomass substitutions (%, thermal basis)	0	25	50	75	100
Biomass burners	/	B41-B46	B31-B36 B41-B46	B21-B26 B31-B36 B41-B46	All
Total burners for biomass	0	6	12	18	24
Coal feed rates (t/h)	79.2	59.4	39.6	19.8	0
Biomass feed rates (t/h)	0	22.5	45.0	67.5	90.1
Primary air (N m^3/h/°C)	201170/100	199726/100	198017/100	196309/100	194600/100
Secondary air (N m^3/h/°C)	224810/289	223196/289	221287/289	219377/289	217468/289
OFA (N m^3/h/°C)	67865/289	67377/289	66801/289	66225/289	65648/289
Protection air (N m^3/h/°C)	26301/289	26112/289	25889/289	25665/289	25442/289
Vertical slot air (N m^3/h/°C)	33105/289	32868/289	32586/289	32305/289	30024/289

study, it is assumed that the nitrogen contained in the char will be directly converted to NO, since its complex conversion mechanisms. Finally, prompt NO also was considered, which is formed by the reaction of atmospheric nitrogen with hydrocarbon radicals in fuel-rich regions of flames [37].

3.5. Discrete phases modeling (DPM)

Both biomass particles and coal particles are modeled by the DPM approach. A key consideration in modeling trajectories of solid fuel is the various forces acting upon the particles. These initial simulations included specific terms for gravitational, buoyancy and drag forces. The trajectories, heat and mass transfer from/to these discrete particles are coupled with the continuous phase. The tra-

Table 4
Kinetic parameters for torrefied biomass and coal particles.

	Torrefied biomass[a]	Coal[b]
Devolatilization kinetics (at high heating rates)		
A1 (s^{-1})	5.48E+03	3.7E+5
A2 (s^{-1})	2.15E+07	1.46E+13
E1 (kJ/mol)	59.8	73.7
E2 (kJ/mol)	147	251
V1	0.62	0.3
V2	0.70	0.8
Char oxidation kinetics		
A (s^{-1})	56.3	0.78
Ea (kJ/mol)	78	94.6

[a] The kinetics of torrefied biomass were measured in this work.
[b] The kinetics of coal were from [30,31].

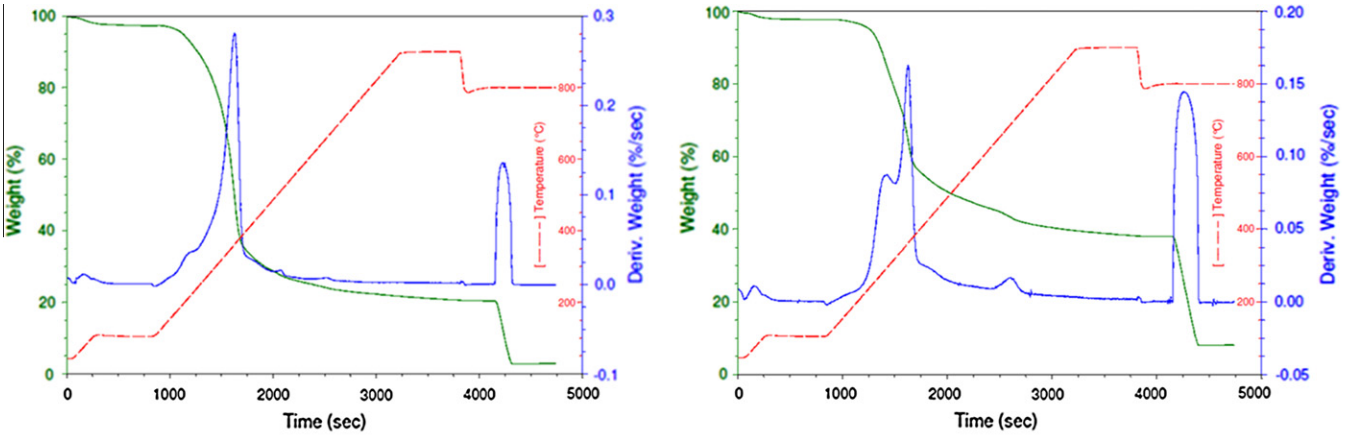

(*a*) Raw biomass (*b*) Torrefied biomass

Fig. 4. TG, DTG and temperature profiles at heating rate of 20 °C/min.

jectory of the discrete phase particle is calculated by integrating the force balance on the particle as motion equations [24]:

$$\frac{du_p}{dt} = \frac{18\mu}{\rho_p d_p^2}\frac{C_D Re}{24}(u - u_p) + \frac{g(\rho_p - \rho)}{\rho_p}$$

3.5.1. Drag force coefficient, C_D

Based on the above equation, obviously, drag force is important for calculating the trajectory of discrete particle. And the drag force coefficient is a function of shape factor of particle [38]. The shape factor Φ, a typical indicator of irregularity of solid particles, was

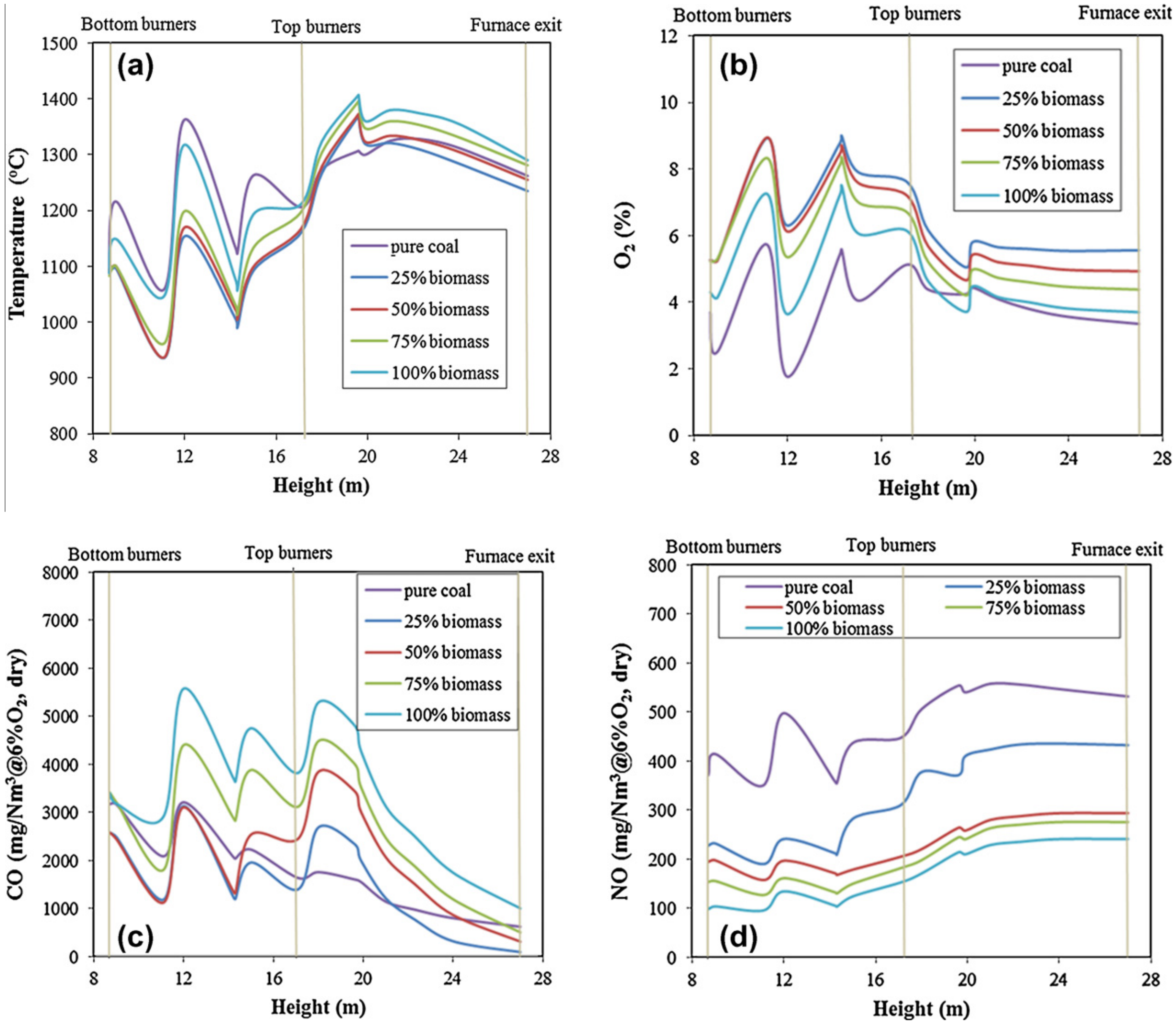

Fig. 5. Profiles of temperature and gas components along the height of boiler.

Table 5
Comparison of heat absorptions in different cases.

	Case 1	Case 2	Case 3	Case 4	Case 5
Biomass substitutions (%)	0	25	50	75	100
Heat absorbed by membrane walls (MW)	229.73	222.29	215.73	206.28	191.47
Heat absorbed by super-heaters (MW)	38.19	44.28	47.15	49.05	50.95
Total heat absorptions (MW)	267.92	266.57	262.88	255.33	242.42
Discrepancies (%)	Base case	−0.50	−1.88	−4.69	−9.52

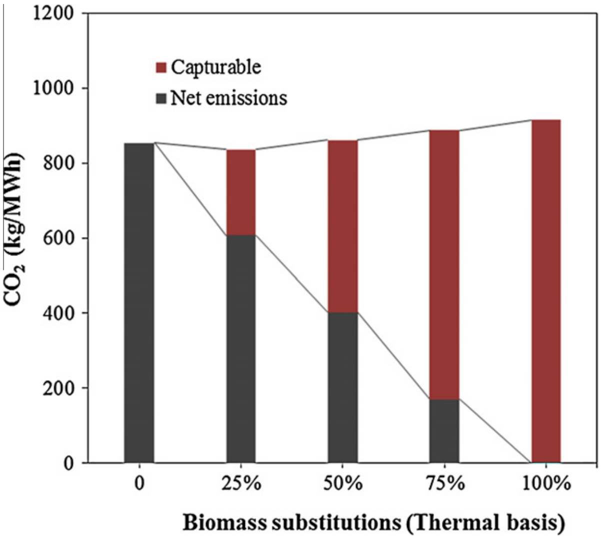

Fig. 6. CO_2 emissions at different substitution ratios of biomass.

defined as a ratio of surface area of a sphere area with the same volume as the particle and the actual surface area. The shape of the biomass particles is affected by the fiber content, although the torrefied biomass has less fiber content, but its surface area is still higher than that of pulverized coal. The higher surface area enhances the drag force imposed onto biomass particles and the contact possibility of O_2 and particle surface. For coal particles, it is widely agreed that the drag force was calculated by spherical drag law [24,39]. In this work, a non-spherical shape was assumed for torrefied biomass particles with a shape factor of 0.54, and the drag coefficient was calculated based on Haider and Levenspiel's equation [38].

3.5.2. Swelling coefficient, C_{SW}

In terms of above equation, the drag force is affected by particle diameter (*dp*). The diameter of a particle changes during devolatilization according to swelling coefficient. The relationship of particle diameter and swelling coefficient is expressed as [24]:

$$\frac{d_p(t)}{d_{p,0}} = 1 + (S_{SW} - 1)\frac{(1 - f_{w,0} - m_p)}{f_{v,0}(1 - f_{w,0})m_{p,0}}$$

where $\frac{(1-f_{w-0})m_{p,0}-m_p}{f_{v,o}(1-f_{w,0}m_{p,0})}$ is the ratio of the mass that has been devolatilized to the total volatile mass of the particle. The effect of swelling on drag force during the biomass devolatilization process should be taken into account, due to the significant fraction of volatile matter in biomass. In this work, swelling coefficient of torrefied biomass particles was also studied experimentally, which was calculated as the ratio of the average diameter of char particles to the average diameter of the initial biomass particles. Finally, the measured swelling coefficient of torrefied biomass is 1.8. According to the experimental studies of Fletcher [40], the swelling coefficient of pulverized coal was selected as 1.1.

4. Results and discussions

4.1. Comparison of torrefied biomass and raw biomass

For comparison, the TG, DTG tests of both raw biomass and torrefied biomass at heating rate of 20 °C/min have been carried out, as shown in Fig. 4. Generally, the first peak of devolatilization is attributed to the hemicellulose decomposition, which is the more reactive chemical compound of biomasses. In Fig. 4, the earlier sub-peak in the DTG curves is at 215 °C for the raw biomass and around 280 °C for the torrefied biomass. The delay of this sub-peak observed in the torrefied materials could be explained in a significant modification of hemicelluloses structure during the torrefaction process. The main peak of devolatilization was observed around 360 °C both for raw biomass and torrefied biomass, which was attributed to the decomposition of cellulose. The decomposition of lignin occurred in a wider range of temperature from 250 °C to the end of the process. Besides, a higher DTG sub-peak of oxidation in torrefied biomass than that in raw biomass shows that torrefaction improved the reactivity of char.

4.2. Kinetic parameters of torrefied biomass

Two competing reactions are used to simulate the devolatilization step and predicted the high temperature volatile matter yield, as above mentioned. Briefly, the first reaction (A1, E1, and V1) are used to prevail at lower temperature, while the second reaction (A2, E2, and V2) plays dominant role at higher temperature. Generally, the volatile matter yield at high temperature is higher than the standard volatile matter revealed. The prediction of the volatile matter yield as function of the temperature is thus important for practice combustion models. The detailed kinetic data for biomass devolatilization are presented in Table 4. Once the pre-exponential factor and activation energy are known, the model provides the rate of volatile evolution and the related char and volatile yields. Finally, the average values of torrefied biomass char oxidation are also listed in Table 4.

4.3. Validation

In this paper, the predicted results of the pure coal case have been compared to the measured values. It is necessary to point out there are some differences between measured values and predicted values due to different positions of them, the measured data were only available before air-preheater, but the predicted results were the Mass-Weight-Average values at the furnace exit. In terms of measured data, average concentrations of O_2, CO, and NO_x were 3.13%, 1124 mg/Nm^3, and 535 mg/N m^3 (at 6% O_2), respectively. The predicted results show good agreements with measured values, and the predicted average concentrations of O_2, and CO were 3.3%, 856 mg/N m^3, and 530 mg/N m^3(at 6% O_2), respectively. In the real condition, the temperature of flue gas exiting the furnace is still high enough for oxidation reactions. Therefore, a lower O_2 content before the air-preheater than at the furnace exit would be reasonable. However, the predicted value of CO concentration was lower than the average of the measured values, probably because the rate of oxidization of carbon in fly ash was faster than the CO consumption rate after the furnace exit. Therefore, it could be concluded that the adopted numerical models in present calculations are reasonable for this study.

4.4. Effects of biomass substitutions on temperature and gas components

Profiles of temperature and main gas components along height of boiler with varying biomass substitutions are shown in Fig. 5. The boiler height used in Fig. 5 starts from the bottom of boiler domain, as shown in Fig. 3. The bottom burners are located on height level of 8.3 m, the top burners are located on height level of 17.1 m, the OFA ports are installed on height level of 19.6 m, and the furnace exit is on height level of 27.6 m.

The comparison of the flue gas temperature is clearly shown along the height of boiler with five different cases in Fig. 5a. Obviously, the flue gas temperatures distributions in those cases are almost shown in the same trends, which might be concluded that chemical properties of torrefied biomass and coal are close, and torrefied biomass can be a good option for replacing coal. From Fig. 5a, the average temperature of the pure coal case was obviously higher than that of co-firing cases in the main combustion chamber (from the bottom burners to the top burners), while after top burners(especially, up to the OFA ports), the average temperatures of co-firing cases were higher than temperature of the coal case. The probably reason is, the motion process was faster than combustion process, due to the enhanced drag force, part of combustible components of biomass was conveyed upwardly to this zone by gas flow. Therefore, the unburned combustibles were oxidized in this zone, which produced a slightly higher temperature in co-firing cases.

The O_2 of air injected into furnace is quickly consumed with the combustion reactions happened, since the temperature inside furnace is enough higher to oxidize the volatile and char of solid fuels. In consequence, the O_2 concentration decreased rapidly after

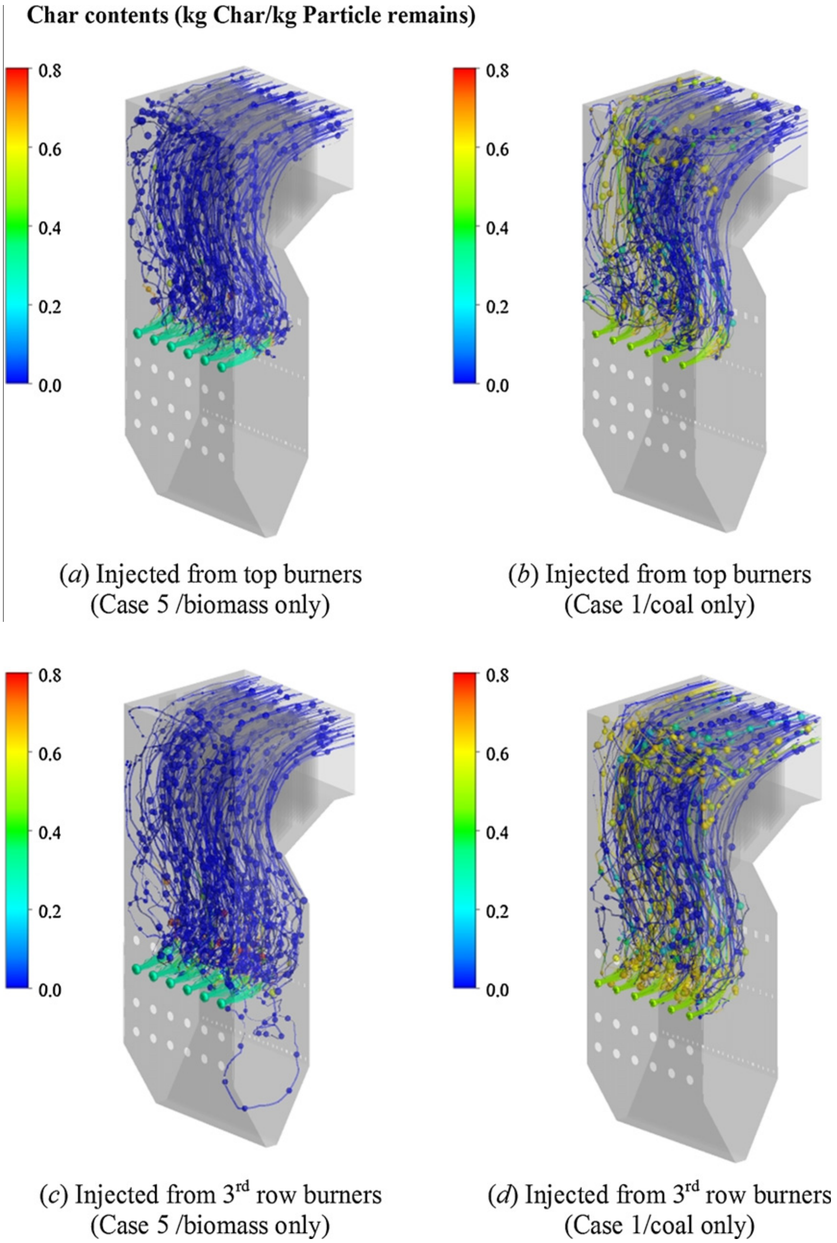

(*a*) Injected from top burners (Case 5 /biomass only)

(*b*) Injected from top burners (Case 1/coal only)

(*c*) Injected from 3rd row burners (Case 5 /biomass only)

(*d*) Injected from 3rd row burners (Case 1/coal only)

Fig. 7. Comparison of char fates and particles trajecoties of biomass case and coal cases.

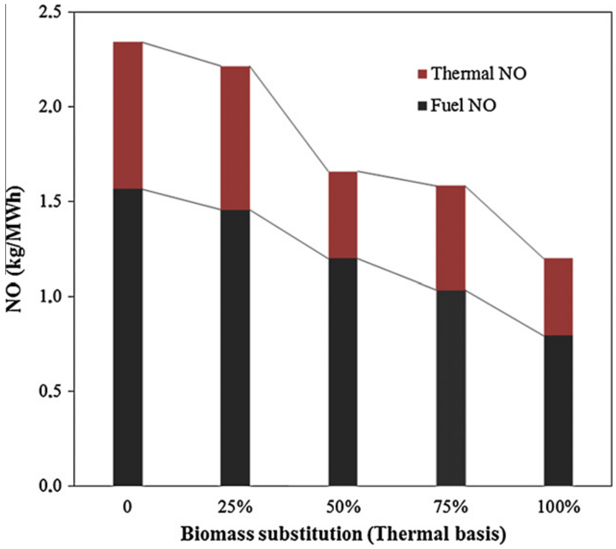

Fig. 8. NO emissions in different substitution ratios of biomass.

injection, as shown in Fig. 5b. In Fig. 5b, the O_2 contents in all co-firing cases were obviously higher in the whole furnace, except the zone close OFA ports. The higher ratios of biomass, the oxygen distribution was more similar with that of the pure coal case. The probable reason is the part of oxygen for biomass combustion was from oxygen content of biomass, so the oxygen devolatilization process from biomass partly slowed down the combustion process of biomass. Compared to coal char, the biomass char was more reactive, but obviously, the content of biomass char was lower. Besides, turbulence flow pattern inside furnace might have some influences on oxygen concentrations in all co-firing cases.

Actually, there are two routes of CO formation, either the oxidation of volatile or char oxidation. The CO concentration on the furnace exit is important to the combustion efficiency of furnace, and a lower CO concentration represents good combustion situation of boiler. The OFA have a significant influence on the CO concentration, which was injected into furnace above burners for complete combustion. Thus, the CO concentration on the furnace exit can be used to judge if the amount of the OFA is enough for complete combustion. The CO concentrations in all cases along the boiler height are shown in Fig. 5c. In Fig. 5c, in all cases, the CO concentrations increased with increasing of biomass substitutions, and a significant reduction was observed after the OFA ports. Interestingly, the CO concentrations in the main furnace zone (from the bottom burners to the top burners) of three co-firing cases and the pure biomass case were higher than that of the pure coal case. Therefore, it can be concluded that the major combustion zone of biomass was moved upwardly to the furnace exit. The reason might be the oxygen devolatilization process from biomass partly slowed down its complete combustion process, because of an important part of oxygen was from biomass itself. The other explanation might be the insufficient gas mixing or stratified flows postponed a part of volatile combustion reactions.

Finally, the characteristics of NO emissions were investigated for all cases. Total NO distributions along the boiler height in all cases are shown in Fig. 5d. It is found that the significant reductions of total NO when switching the coal as torrefied biomass. Especially, the reduction of NO emissions is more clearly when the 50% of biomass on thermal basis was used in co-firing system. It seems that the thermal NO mostly formed in the upper zone of boiler since the slightly higher temperature when considered the temperature distribution in Fig. 5a, but simultaneously, it should be acknowledged that the short residence time of flue gas in the upper zone limited the formation of thermal NO, because the temperature of fuel gas was then quickly cooled down by the super-heaters. Moreover, the overall fuel-N contents decreased with increasing of biomass substitutions, due to the lower nitrogen content of biomass compared to coal. Additionally, the fuel nitrogen in biomass volatile was mostly converted to NH_3, which has a lower conversion ratio of NO when compared to HCN [7].

4.5. Effects of biomass substitutions on boiler efficiency

Boiler load reduces when coal-fired boiler operated as co-firing mode, due to biofuel has a high water content [4]. When directly using a high moisture biofuel, the overall energy efficiency of the co-firing plant would be reduced unexpectedly. The process of torrefaction moves the chemical and physical properties of the raw biomass close to that of bituminous coal with releasing almost all the moisture and less part of volatiles, which is expected to realize high biomass co-firing ratios without reducing energy efficiency. Therefore, the thermal performance of a torrefaction based co-firing boiler has been investigated in this work.

Generally, a lower boiler load reduces the heat absorption of installed heat exchangers, and therefore the temperature and pressure of main steam. In this work, to analysis the fluctuations of the boiler loads when the torrefied biomass replaced coal with varying biomass substitutions, the heat absorbed by the membrane walls and the super-heaters in different cases have been investigated and compared, as given in Table 5. The absorbed heat is defined as the integrations of heat flux over the whole area of studied walls/surfaces. In all cases, constant temperatures were kept as thermal boundary conditions of both the membrane walls and the super-heaters. From Table 5, it is observed that a relative less heat absorbed by membrane walls and a relative more heat absorbed by super-heaters at a higher biomass substitution. This might be caused by the major combustion zone of biomass was moved upwardly to furnace exit, as discussed before. The discrepancies of total heat absorptions are also listed in Table 5. The largest discrepancy of −9.52% was found in the pure biomass case when compared to the pure coal case, which means that no more than 10% of boiler load was reduced if 100% coal was replaced by the torrefied biomass. Consequently, torrefied biomass provides a promising co-firing option with a higher boiler efficiency and minor fluctuation of the boiler load.

4.6. Effects of biomass substitutions on CO_2 emissions

Biomass is an important renewable resource and the CO_2 released during biomass combustion will be re-captured by the re-growth of the biomass through photosynthesis [41,42]. CO_2 emission from the combustion of biomass fuel source is not assumed to increase the net atmospheric CO_2 levels [42]. Therefore, biomass is widely accepted as a potential solid fuel to reduce the net emission of CO_2. Typically, a large subcritical coal-fired utility plant produce 900 kgCO_2/MW h, and 750 kg CO_2/MW h for a supercritical plant [43]. To understand the different fates of CO_2, capturable CO_2 and net CO_2 with unit of kg/MW h were compared based on the predicted data, as shown in Fig. 6. It is defined that the capturable CO_2 derives from biomass combustion and the net CO_2 origins from coal combustion. Fig. 6, as expected, shows that the net CO_2 reduces with increasing biomass percentages, while the capturable CO_2 increases simultaneously. There are 915 kg CO_2/MW h recaptured when 100% coal substituted by the torrefied biomass. When 50% of biomass used in the co-firing boiler, the emission of net CO_2 is 403 kg/MW h, which is less than half of emission of the net CO_2 in the pure coal case.

Moreover, the total CO_2 emission of the pure biomass case and three co-firing cases are slightly higher than that of the pure coal case. Firstly, because the total energy inputs of fuel are same for all cases (see 3.2). According to the proximate and ultimate analyses of coal and torrefied biomass, it can be theoretically calculated that the total carbon content of fuel in the pure biomass case is slightly higher than that in the pure coal case. Secondly, the unburned carbon contents in biomass ash were less than that of coal ash, since the biomass char is more reactive compared to coal char. It is commonly acknowledged that the surface combustion of biomass char is much faster than of pulverized coal, due to enhanced mass transfer and intrinsic reaction kinetics. According to the prediction, the char burnout ratios of biomass in all co-firing cases were 100% and the total char burnout ratio for the pure biomass case was 99.95%, while the total char burnout ratio of coal for the pure coal case was 97.75%. For clarify, the char contents of biomass and coal particles and their trajectories are clearly presented in Fig. 7. The biomass particles were almost combusted completely before leaving the domain when injected from top two rows burners; while coal particles showed similar trajectories, but the unburned carbon in coal ash is higher than that of biomass ash.

4.7. Effects of biomass substitutions on NO emissions

This substitution of biomass also has the potential to reduce the emission of air pollutants. Particularly, the emissions of NO_x, which mainly due to the lower nitrogen content in the biomass. Fig. 8 shows the NO emissions with varying substitution ratios of biomass. Obviously, the emissions of the fuel NO showed a linear and decreased with increasing of substitutions of biomass, and ratios of thermal NO/fuel NO were almost same in all cases, except the sudden decreasing of thermal NO at 50% biomass case. Therefore, in general, the total NO emission reduced with biomass substitution increasing. The total NO emission based on power output was 2.34 kg/MW h in the pure coal case, and almost half amount of which was reduced when 100% coal replaced by the torrefied biomass.

To further understand the emission characteristics of the NO with varying biomass percentages in co-firing system, the formation rate of thermal NO and fuel NO were studied separately, as shown in Fig. 9. It is observed that both the fuel NO and the thermal NO were mostly formed within an envelope of flames, since

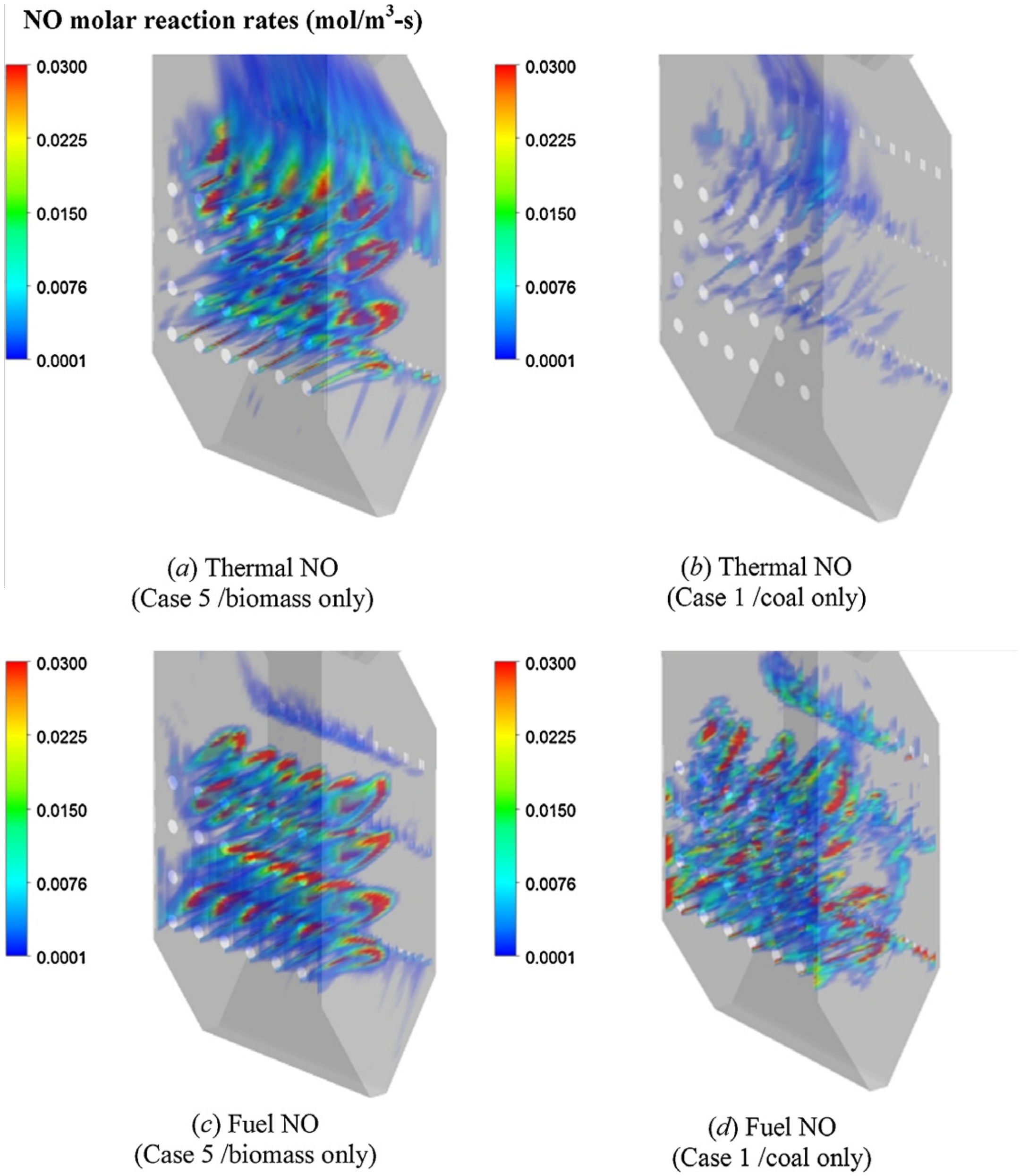

(*a*) Thermal NO
(Case 5 /biomass only)

(*b*) Thermal NO
(Case 1 /coal only)

(*c*) Fuel NO
(Case 5 /biomass only)

(*d*) Fuel NO
(Case 1 /coal only)

Fig. 9. Comparison of NO molar reaction rates of biomass case and coal cases.

their formation rates primarily depend on the temperature and fuel/oxygen ratio. Near the burner region, due to the temperature of solid fuel rose up suddenly, the NH_3 or HCN were formed rapidly with releasing of the volatiles. Both in the pure biomass and the pure coal cases, the volumes with thermal NO formation rates above 0.0001 mol/m^3-s are observed in the upper-center of the furnace when compared with that of fuel NO formation rates, as shown in Fig. 9, which means that an important part of the thermal NO was formed in the zone of above burners, where the intermediates of the volatile-N subsequently reacted to form NO_x under an oxidizing environment, because the OFA was injected proving the completely combustion air, but resulted in a lower emission of fuel NO. The size of the zone for the thermal NO formation rate was smaller compared to that of the fuel NO_x formation for the pure coal case, which was similar with numerical results of Choi and Kim [44], this might because of the fuel NO formed more readily than the thermal NO during the coal combustion process. However, compared to the pure coal case, thermal NO/fuel NO ratios increased with gradually increasing of the coal replaced by the torrefied biomass, which can also be observed from Fig. 8. Furthermore, the major formation rates of the fuel NO in the pure biomass case showed a good corresponding to the envelope of flame, while the formation rate of the fuel NO in the pure coal case showed less order, as shown in Fig. 9c and d.

5. Conclusions

A torrefaction based co-firing system was proposed and studied systematically in this work. Torrefied biomass has several benefits, such as higher energy density, good grindability, higher flowability and uniformity in product quality. The process of torrefaction moves the chemical and physical properties of raw biomass close to that of bituminous coal, which allows co-utilization with high substitution ratios of biomass in the existing coal-fired boilers without major modifications. CFD modeling of torrefaction based co-firing system in a pulverized coal boiler has been carried out with the aim of 100% fuel switching. To figure out the performance of co-firing of torrefied biomass in a front-wall pulverized coal boiler, five different cases were involved and simulated, coal only, 25% biomass, 50% biomass, 75% biomass, and 100% biomass, respectively.

According to the results, torrefaction is bale to provide a technical option for high substitutions of biomass in the co-firing system. The case-study boiler can be operated with a higher substitution ratio of substitution of the torrefied biomass without obvious decreasing of energy efficiency and fluctuation of boiler load. More positively, the net CO_2 and the NO_x emissions significantly reduced with increasing of biomass substitutions. However, torrefaction based the co-firing system should be further studied from perspective of other common issues, such as fouling, corrosion of the boiler, fly ash utilization, impacts on performance of the flue gas cleaning, and so on. In addition, the torrefaction based co-firing system also should be evaluated according to economic criteria for application.

Acknowledgement

The authors would like to thank EU/KIC-Innoenergy and Ind-Comb AB, Sweden for the financial support of this work.

References

[1] Munir S, Nimmo W, Gibbs BM. The effect of air staged, co-combustion of pulverised coal and biomass blends on NO_x emissions and combustion efficiency. Fuel 2011;90(1):126–35.

[2] Nussbaumer T. Combustion and co-combustion of biomass: fundamentals, technologies, and primary measures for emission reduction. Energy Fuels 2003;17(6):1510–21.

[3] http://ec.europa.eu/environment/air/pdf/final_report_05225.pdf.

[4] Basu P, Butler J, Leon MA. Biomass co-firing options on the emission reduction and electricity generation costs in coal-fired power plants. Renew Energy 2011;36(1):282–8.

[5] Al-Mansour F, Zuwala J. An evaluation of biomass co-firing in Europe. Biomass Bioenergy 2010;34(5):620–9.

[6] Kati S. Co-firing of biomass in coal-fired utility boilers. Appl Energy 2003;74(3–4):369–81.

[7] Karampinis E et al. Numerical investigation Greek lignite/cardoon co-firing in a tangentially fired furnace. Appl Energy 2012;97:514–24.

[8] Pallarés J et al. Numerical study of co-firing coal and Cynara cardunculus in a 350 MWe utility boiler. Fuel Process Technol 2009;90(10):1207–13.

[9] Dong C et al. Numerical modeling of the gasification based biomass co-firing in a 600 MW pulverized coal boiler. Appl Energy 2010;87(9):2834–8.

[10] Kalisz S, Pronobis M, Baxter D. Co-firing of biomass waste-derived syngas in coal power boiler. Energy 2008;33(12):1770–8.

[11] Mory A, Zotter T. Eu-demonstration project BioCoComb for biomass gasification and co-combustion of the product-gas in a coal-fired power plant in austria. Biomass Bioenergy 1998;15(3):239–44.

[12] Maciejewska A, Veringa H, Sanders J, Peteves SD. Co-firing of biomass with coal constraints and role of biomass pre-treatment. European Commission; 2006.

[13] Bergman PCA, et al. Torrefaction for biomass co-firing in existing coal-fired power stations. In: ECN-C-05-0132005.

[14] Arias B et al. Influence of torrefaction on the grindability and reactivity of woody biomass. Fuel Process Technol 2008;89(2):169–75.

[15] Kongkeaw N, Patumsawad S. Thermal upgrading of biomass as a fuel by torrefaction. In: Second international conference on environmental engineering and applications. Singapore: IACSIT Press; 2011. p. 38–42.

[16] Hakkou M et al. Investigations of the reasons for fungal durability of heat-treated beech wood. Polym Degrad Stab 2006;91(2):393–7.

[17] Prins MJ, Ptasinski KJ, Janssen FJJG. Torrefaction of wood: Part 1. Weight loss kinetics. J Anal Appl Pyrol 2006;77(1):28–34.

[18] Prins MJ, Ptasinski KJ, Janssen FJJG. Torrefaction of wood: Part 2. Analysis of products. J Anal Appl Pyrol 2006;77(1):35–40.

[19] Uslu A, Faaij APC, Bergman PCA. Pre-treatment technologies, and their effect on international bioenergy supply chain logistics. Techno-economic evaluation of torrefaction, fast pyrolysis and pelletisation. Energy 2008;33(8):1206–23.

[20] Repellin V et al. Energy requirement for fine grinding of torrefied wood. Biomass Bioenergy 2010;34(7):923–30.

[21] Svoboda K et al. Pretreatment and feeding of biomass for pressurized entrained flow gasification. Fuel Process Technol 2009;90(5):629–35.

[22] Biagini E, Biasci L, Tognotti L. Biomass characterisation-data report; 2012.

[23] Li J et al. CFD approach for unburned carbon reduction in pulverized coal boilers. Energy Fuels 2011;26(2):926–37.

[24] Ansys. Ansys fluent 12.0-theory guide; 2009.

[25] Launder BE, Spalding DB. The numerical computation of turbulent flows. Comput Methods Appl Mech Eng 1974;3(2):269–89.

[26] Smoot LD, Pratt DT. Pulverized-coal combustion and gasification theory and applications for continuous flow processes. New York: Plenum Press; 1979.

[27] Kobayashi H, Howard JB, Sarofim AF. Coal devolatilization at high temperatures. Symposium (international) on combustion, 1977;16(1):411–25.

[28] Baum MM, Street PJ. Predicting the combustion behaviour of coal particles. Combust Sci Technol 1971;3(5):231–43.

[29] Field MA. Rate of combustion of size-graded fractions of char from a low-rank coal between 1200 K and 2000 K. Combust Flame 1969;13(3):237–52.

[30] Li ZQ, Wei F, Jin Y. Numerical simulation of pulverized coal combustion and NO formation. Chem Eng Sci 2003;58(23–24):5161–71.

[31] Hurt RH, Mitchell RE. Unified high-temperature char combustion kinetics for a suite of coals of various rank. Symposium (international) on combustion, 1992;24(1):1243–50.

[32] Morgan ME, Roberts PA. Coal combustion characterisation studies at the international flame research foundation. Fuel Process Technol 1987;15:173–87.

[33] Field MA et al. Combustion of pulverized coal. Ind Eng Chem 1969;61(3):8–9.

[34] De Soete GG. Overall reaction rates of NO and N_2 formation from fuel nitrogen. Symposium (international) on combustion 1975;15(1):1093-102.

[35] Winter F et al. The NO and N_2O formation mechanism during devolatilization and char combustion under fluidized-bed conditions. Symposium (international) on combustion, 1996;26(2):3325–34.

[36] Liu H, Gibbs BM. Modelling of NO and N_2O emissions from biomass-fired circulating fluidized bed combustors. Fuel 2002;81(3):271–80.

[37] Fenimore CP. Reactions of fuel-nitrogen in rich flame gases. Combust Flame 1976;26:249–56.

[38] Haider A, Levenspiel O. Drag coefficient and terminal velocity of spherical and nonspherical particles. Powder Technol 1989;58(1):63–70.

[39] Morsi SA, Alexander AJ. An investigation of particle trajectories in two-phase flow systems. J Fluid Mech 1972;55(02):193–208.

[40] Fletcher TH. Swelling properties of coal chars during rapid pyrolysis and combustion. Fuel 1993;72(11):1485–95.

[41] Zhang L, Xu C, Champagne P. Overview of recent advances in thermo-chemical conversion of biomass. Energy Convers Manage 2010;51(5):969–82.

[42] http://www.bipac.net/afpa/AFPACarbonNeutralityWhitePaper2_4_10.pdf.

[43] IEA. Power generation from coal: measuring and reporting efficiency performance and CO_2 emissions; 2010.

[44] Choi CR, Kim CN. Numerical investigation on the flow, combustion and NO_x emission characteristics in a 500 MWe tangentially fired pulverized-coal boiler. Fuel 2009;88(9):1720–31.